

Dynamic simulations of the Kosterlitz-Thouless phase transition

B. Zheng,^{1,2} M. Schulz,¹ and S. Trimper¹

¹Universität Halle, 06099 Halle, Germany

²Universität GH Siegen, 57068 Siegen, Germany

(Received 19 August 1998)

Based on the short-time dynamic scaling form, a dynamic approach is proposed to numerically tackle the Kosterlitz-Thouless phase transition. Taking the two-dimensional XY model as an example, the exponential divergence of the spatial correlation length, the transition temperature T_{KT} , and all critical exponents are computed. Compared with Monte Carlo simulations in equilibrium, we obtain data at temperatures closer to T_{KT} . [S1063-651X(99)50802-7]

PACS number(s): 02.70.Lq, 75.10.Hk, 64.60.Fr, 64.60.Ht

The Kosterlitz-Thouless (KT) phase transition is an important kind of phase transition in nature [1,2]. When the temperature approaches the transition temperature T_{KT} from above, the spatial correlation length diverges *exponentially*, rather than by a power law in a second order phase transition. Below T_{KT} , the system remains *critical* in the sense that the spatial correlation length is divergent. No real long range order emerges in the whole temperature regime. Important examples of systems with a KT transition are the classical XY -type models, quantum Heisenberg models, hard disk models, and other relevant fluid systems as well as field theories.

It is well known that due to the exponential divergence at the transition temperature, numerical simulations of critical systems with a KT transition suffer severely from critically slowing down. For example, to compute the spatial correlation length of the two-dimensional classical XY model, even with the cluster algorithm and the over-relaxed algorithm, one has only reached the temperature $T=0.98$, which is still fairly far from T_{KT} , estimated to be around 0.89 to 0.90 [3–5]. If some quenched randomness is added to the system, e.g., in the fully frustrated XY model, the situation becomes even more complicated [6–10].

Recently much progress has been made in critical dynamics. It has been discovered that universal dynamic scaling behavior already emerges in the *macroscopic* short-time regime, after a microscopic time scale t_{mic} [11–19]. More interesting and important is that the static exponents, originally defined in equilibrium, enter the short-time dynamic scaling. This provides a possible way for extracting these exponents from the short-time dynamic scaling behavior [19]. Since the measurements are carried out in the macroscopic short-time regime, the method is free from critical slowing down.

Such a short-time dynamic approach has been systematically investigated for critical dynamic systems with a *second order* phase transition. It has been verified in the simple Ising and Potts model [20,21] and recently applied successfully to general and complex systems as nonequilibrium dynamic systems [22,23], the chiral degree of freedom in the fully frustrated XY model [24], and lattice gauge theory [25]. The critical exponents as well as the critical temperature can be extracted either from the power law behavior of the observables at the early times or from the finite size scaling. Compared with the nonlocal cluster algorithms, the dynamic approach does study the dynamic properties of the original local dynamics.

However, it is not clear whether the short-time dynamic approach can systematically go beyond critical systems with a second order phase transition, even though an attempt has been made with the KT transitions and the spin glass transitions [26–29]. For systems with a KT transition, for example, owing to the *absence* of symmetry breaking and to the fact that the system remains critical below T_{KT} , a clear signal as for a second order phase transition [21,19,24] does not exist for the transition temperature T_{KT} . The exponent ν and T_{KT} have not been determined. Standard techniques developed for the second order phase transitions do not apply here. On the other hand, besides the exponents, whether one can obtain other critical properties of the equilibrium state, especially the spatial correlation length from the short-time dynamics, remains unknown, even for *second order* phase transitions.

In this Rapid Communication we propose a short-time dynamic approach to the KT transition using the two-dimensional XY model as an example. From the short-time dynamic scaling, we extract the *spatial correlation length* of the equilibrium state. From the spatial correlation length we estimate the transition temperature T_{KT} and the static exponent ν . With T_{KT} at hand, the static exponent η and dynamic exponent z are obtained from power law behavior of the magnetization and Binder cumulant. Our choice for the XY model was based solely on the substantial amount of comparative data concerning Monte Carlo simulations in equilibrium.

The XY model in two dimensions is defined by the Hamiltonian

$$H = \frac{1}{T} \sum_{\langle ij \rangle} \vec{S}_i \cdot \vec{S}_j, \quad (1)$$

where $\vec{S}_i = (S_{i,x}, S_{i,y})$ is a planar unit vector at site i and the sum is over the nearest neighbors. In our notation, the coupling constant is already absorbed in the temperature. Large scale Monte Carlo simulations in equilibrium have been performed to understand the properties of the phase transition [3–5]. The spatial correlation length ξ and susceptibility χ have been calculated in a temperature interval [0.98,1.43] with lattice sizes up to 512. The results support a KT singularity for the spatial correlation length

$$\xi(\tau) \sim \exp(b\tau^{-\nu}) \quad (2)$$

TABLE I. Our results of the exponents and T_{KT} obtained in the temperature interval $[T_1, T_2]$ in comparison with those in Ref. [5] (denoted by †). T_{KT}^* and ν^* of Ref. [5] are from data of the susceptibility. The second and fourth columns are the results with a fixed $\nu = 0.5$ as input. Our values of z and η are measured at $T_{KT} = 0.894$ and η of Ref. [5] is estimated with finite size scaling and Monte Carlo renormalization group methods at $T_{KT} = 0.894$ also. bz for Ref. [5] is calculated by taking our z as input.

$[T_1, T_2]$	[0.94, 1.07]	[0.94, 1.07]	[0.98, 1.43]†	[0.98, 1.43]†
T_{KT}	0.8942	0.8926	0.8953	0.8914
bz	4.12	3.82	3.67	3.38
ν	0.48	0.5	0.47	0.5
T_{KT}^*			0.8871	0.8961
ν^*			0.57	0.5
z	1.96(3)			
η	0.238(4)		0.235(5)	

and for the susceptibility $\chi(\tau) \sim \xi^{2-\eta}(\tau)$, with $\tau \sim (T - T_{KT})/T_{KT}$ as the reduced temperature. However, unconstrained four-parameter fits to the data do not yield completely satisfactory results [5]. The measured values of ν and T_{KT} from the data of ξ and χ are not very consistent and stable. η estimated from $\chi(\tau) \sim \xi^{2-\eta}(\tau)$ is above 0.7 and too big compared with the theoretical prediction $\eta = 0.25$. The temperatures for the available data of ξ and χ are still far from the transition temperature T_{KT} estimated to be around 0.89–0.90 (for details, see Table I and Ref. [5]). However, simulations in equilibrium with lower temperatures are very difficult.

We will demonstrate that from the short-time dynamic scaling, the spatial correlation length $\xi(\tau)$ of the equilibrium state can be extracted with relatively small lattices. This is because the *nonequilibrium* spatial length $\xi(t, \tau)$ is small in the short-time regime of the dynamic evolution. Therefore, simulations can be performed at lower temperatures.

In this paper we consider only the dynamics of model A, which is relaxational without energy and magnetization conservation. Starting from an *ordered* initial state, e.g., all $\vec{S}_i = (S_{i,x}, S_{i,y}) = (1, 0)$, the system is updated at the temperature above T_{KT} with the *standard Metropolis algorithm*. We stop updating at a certain Monte Carlo time t_m and repeat the procedure. Total samples for average is from 800 to 1200 for lattice size $L = 256$ and above 400 for $L = 512$. The lattice size $L = 256$ is used in simulations for temperatures from $T = 1.07$ down to 0.975, while $L = 512$ from $T = 0.97$ to 0.94. Extra simulations with other lattice sizes confirm that our data have no visible finite size effect.

The observable we measure is the magnetization defined as

$$M(t) = \frac{1}{L^d} \left\langle \sum_i S_{i,x}(t) \right\rangle. \quad (3)$$

From a general physical view point of the renormalization group transformation, the magnetization $M(t)$ is subject to a scaling form

$$M[t, \xi(\tau)] = t^{-\eta/2z} M[1, t^{-1/z} \xi(\tau)]. \quad (4)$$

When the temperature is at T_{KT} (or below), i.e., $\tau = 0$, $\xi(\tau) \rightarrow \infty$, and $M(t)$ undergoes a power law decay, $M(t) \sim t^{-\eta/2z}$. However, for $\tau > 0$, the power law behavior is

modified by the scaling function $M[1, t^{-1/z} \xi(\tau)]$. This fact can be used for the determination $\xi^z(\tau)$ and the exponent η/z .

In Fig. 1, the time evolution of the magnetization is displayed on a log-log scale for different temperatures. We perform Monte Carlo simulations up to a time t_m where there is visible deviation from the power law behavior. Actually, in the short-time regime of the dynamic evolution, the magnetization itself is more or less self-averaged. We may increase the lattice size without too much extra fluctuation. What restricts our simulations to very low temperatures is only t_m . Our longest updating time is $t_m = 50\,000$ at the temperature $T = 0.94$. To obtain the curve for $T = 0.98$, one needs eight days in ALPHA station 500 (400 MHz), while ten times more for $T = 0.94$.

Now from a scaling collapse of two curves with a pair of temperatures (T_1, T_2) , we estimate the ratio ξ_1^z/ξ_2^z and η/z . Here ξ_1 and ξ_2 are the values of $\xi(\tau)$ at the temperatures T_1 and T_2 , respectively. In Fig. 2, such a scaling plot is displayed for $(T_1, T_2) = (0.955, 0.965)$. We multiply the magnetization $M(t_1, \xi_1)$ by an overall factor b^α and rescale t_1 to t_1/b . According to the scaling form (4) this rescaled $M(t_1, \xi_1)$ is equal to $M(t_2, \xi_2)$ if and only if $b = \xi_1^z/\xi_2^z$ and

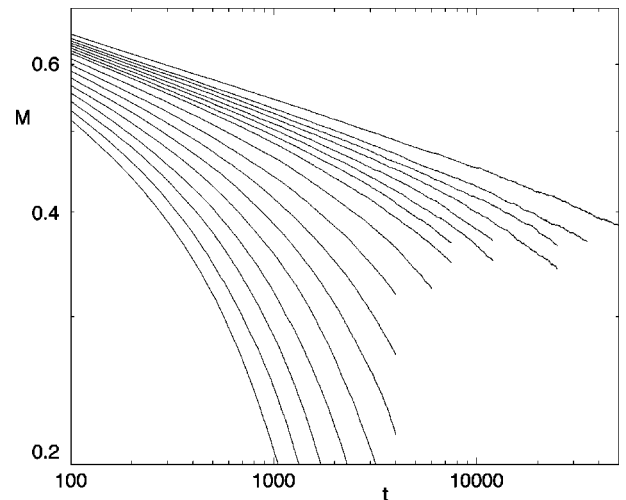


FIG. 1. Time evolution of the magnetization in the log-log scale. The temperatures are 0.94, 0.95, 0.955, 0.96, 0.965, 0.97, 0.975, 0.98, 0.99, 1.00, 1.01, 1.02, 1.03, 1.04, 1.05, 1.06, and 1.07 (from above).

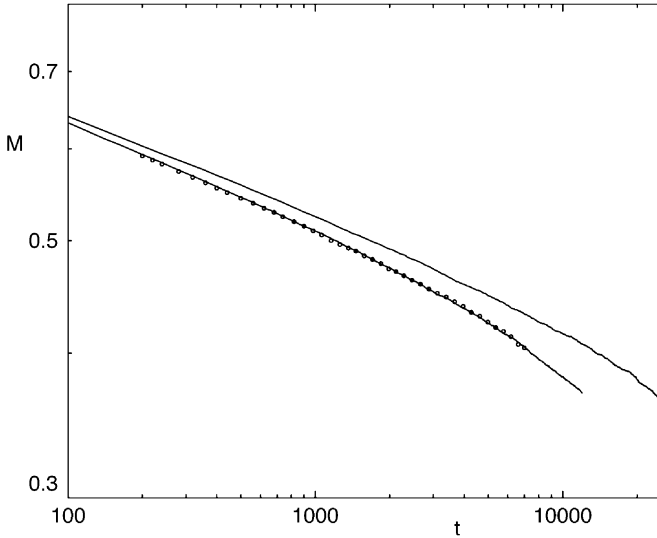


FIG. 2. Scaling plot of the magnetization with a pair of temperatures (T_1, T_2) . The upper and lower solid lines correspond to temperatures $T_1=0.955$ and $T_2=0.965$. The circles are also the magnetization with $T_1=0.955$, but are rescaled to have the best fit with that of $T_2=0.965$.

$\alpha = \eta/2z$. Therefore, searching for the best fit between $M(t_2, \xi_2)$ and the rescaled $M(t_1, \xi_1)$, we determine ξ_1^z/ξ_2^z and $\eta/2z$. In the figure, the circles represent the rescaled $M(t_1, \xi_1)$ best fitted to $M(t_2, \xi_2)$.

Theoretically, the exponents η and z are defined at the transition temperature T_{KT} . The exponent ν and the exponential singularity in Eq. (2) are defined for temperatures above, but in the close neighborhood, of T_{KT} . If the temperature is fairly above T_{KT} , in principle, all the exponents and the parameters b may have some dependence on the temperature. Usually this dependence on the temperature is neglected, otherwise the situation becomes too complicated

[5]. In our dynamic approach, we perform the scaling collapse of the magnetization with two temperatures that are not too far away from each other and therefore the dependence of η/z on the temperature is actually considered. However, we assume ν and bz to be independent of the temperature.

In Table II, the measured ratio of ξ_1^z/ξ_2^z and exponent $\eta/2z$ for different pairs of temperatures (T_1, T_2) are listed. Errors are estimated by dividing the total samples for the time-dependent magnetization into two groups only. The lowest temperature we reach is $T=0.94$. For comparison, in Table II available values of ξ_1^z/ξ_2^z from Ref. [5] (denoted by \dagger) are also given. They are slightly smaller than our results. We observe that, as the temperature decreases, these values of ξ_1^z/ξ_2^z do not increase sufficiently smoothly. Real errors of these data (and also our data) might be somehow bigger than given in the table. Taking $z=1.96$ in Table I as input, the resulting η from $\eta/2z$ in Table II is around 0.26 to 0.31. As expected [5], we see a tendency that η will become approximately 0.25 as the temperature approaches T_{KT} .

Now we fit the data in Table II to the exponential form in Eq. (2) and estimate the transition temperature T_{KT} , the exponent ν , and the parameter bz . The best results are given in Table I in comparison with those from simulations in equilibrium. Our results are fitted from a relatively lower temperature interval [0.94, 1.07], and agree well with those obtained in a temperature interval [0.98, 1.43] in Ref. [5], in both cases of an unconstrained fit and a fit with a fixed $\nu=0.5$. However, as pointed out by the authors of Refs. [5, 4], for the unconstrained fit, the minimum in the parameter space is not very stable in the directions of ν and bz . It is somehow by chance that our value of $\nu=0.48$ is so close to $\nu=0.47$ obtained in Ref. [5]. When we vary T_2 in the fitting interval $[0.94, T_2]$ from 1.07 to smaller values, the exponent ν first drops down and then rises again after around $T_2=1.00$. These fluctuations very probably come from the fact that we do not have sufficient data points and accuracy for

TABLE II. Measured ratio ξ_1^z/ξ_2^z and exponent $\eta/2z$ for different pairs of temperatures. Values of ξ_1^z/ξ_2^z are calculated from data in Table VIII of Ref. [5].

(T_1, T_2)	(0.940, 0.950)	(0.950, 0.955)	(0.950, 0.960)	(0.955, 0.960)	(0.955, 0.965)	(0.960, 0.965)
ξ_1^z/ξ_2^z	5.75(38)	2.04(06)	3.61(07)	1.81(09)	3.05(06)	1.65(04)
$\eta/2z$	0.0680(11)	0.0695(16)	0.0690(17)	0.0682(21)	0.0674(12)	0.0650(21)
(T_1, T_2)	(0.960, 0.970)	(0.965, 0.970)	(0.965, 0.975)	(0.970, 0.975)	(0.97, 0.98)	(0.97, 0.99)
ξ_1^z/ξ_2^z	2.65(07)	1.56(03)	2.35(02)	1.51(01)	2.165(45)	4.35(11)
$\eta/2z$	0.0671(21)	0.0691(18)	0.0676(12)	0.0685(08)	0.0682(17)	0.0699(22)
(T_1, T_2)	(0.975, 0.98)	(0.98, 0.99)	(0.98, 1.00)	(0.99, 1.00)	(0.99, 1.01)	(1.00, 1.01)
ξ_1^z/ξ_2^z	1.47(03)	1.965(43)	3.67(07)	1.840(40)	3.22(06)	1.710(22)
ξ_1^z/ξ_2^z \dagger		1.839(84)		1.605(61)		1.600(39)
$\eta/2z$	0.0668(20)	0.0727(28)	0.0768(15)	0.0753(22)	0.0774(14)	0.0762(26)
(T_1, T_2)	(1.00, 1.02)	(1.01, 1.02)	(1.01, 1.03)	(1.02, 1.03)	(1.02, 1.04)	(1.03, 1.04)
ξ_1^z/ξ_2^z	2.690(29)	1.564(08)	2.334(21)	1.474(10)	2.131(20)	1.424(07)
ξ_1^z/ξ_2^z \dagger		1.453(36)		1.434(34)		1.351(38)
$\eta/2z$	0.0784(24)	0.0781(11)	0.0768(19)	0.0773(13)	0.0777(11)	0.0754(16)
(T_1, T_2)	(1.03, 1.05)	(1.04, 1.05)	(1.04, 1.06)	(1.05, 1.06)	(1.05, 1.07)	(1.06, 1.07)
ξ_1^z/ξ_2^z	1.964(17)	1.380(07)	1.832(19)	1.329(10)	1.726(13)	1.312(6)
$\eta/2z$	0.0778(18)	0.0835(42)	0.0777(12)	0.0705(46)	0.0781(19)	0.0900(24)

each data point. The estimate of T_{KT} is relatively stable. However, the impression is that the value of T_{KT} might be slightly bigger than $T_{KT}=0.8942$, given in the table, if the fitting can confidently be performed in the really close neighborhood of T_{KT} .

With the transition temperature T_{KT} at hand, we proceed to measure the magnetization M and its second moment $M^{(2)}$ at T_{KT} . To seek the dynamic exponent z , we construct a Binder cumulant $U = M^{(2)}/M^2 - 1$. Finite size scaling analysis leads to the short-time behavior [26,19,24]

$$U(t) \sim t^{d/z}. \quad (5)$$

Finally, an accurate value of $\eta/2z$ can be obtained from the power law decay of the magnetization $M(t) \sim t^{-\eta/2z}$ [see Eq. (4)]. In Fig. 3, $M(t)$ and $U(t)$ have been plotted on a log-log scale. Since our measurements only extend to $t=750$, a lattice size $L=64$ is sufficient. Total samples for average are 12 000. From the slopes of the curves in the figure we measure d/z and $\eta/2z$, then calculate z and η . The results are included in Table I. Our $\eta=0.238(4)$ coincides with the best estimate $\eta=0.235(5)$ in equilibrium.

In conclusion, a dynamic approach is proposed to numerically tackle the Kosterlitz-Thouless phase transition. We demonstrate that not only the critical exponents but also the spatial correlation length of the equilibrium state can be obtained from the short-time dynamics. Taking the two-dimensional XY model as an example, the exponential divergence of the spatial correlation length is extracted from the short-time dynamic scaling. The transition temperature T_{KT} , the static exponents ν and η , as well as the dynamic exponent z , are then estimated. Since the measurements are carried out in the short-time regime of the dynamic evolution,

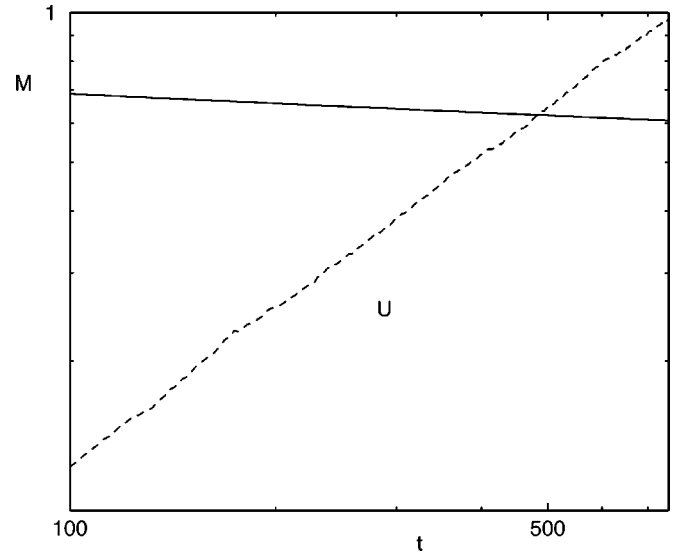


FIG. 3. Time evolution of the magnetization M and Binder cumulant U at $T_{KT}=0.894$ in the log-log scale. To plot the figure U has been multiplied by a constant 200.

where the *nonequilibrium* spatial correlation length is small, we do not encounter the difficulties of generating independent configurations. Compared with the simulations in equilibrium, we can perform simulations at the temperatures closer to T_{KT} . This method can, in principle, be applied or generalized to other kinds of phase transitions as second order phase transitions and spin glass transitions.

The work was supported in part by the Deutsche Forschungsgemeinschaft under Grant Nos. Schu 95/9-1 and SFB 418.

-
- [1] J. M. Kosterlitz and D. J. Thouless, *J. Phys. C* **6**, 1181 (1973).
 - [2] J. Kosterlitz, *J. Phys. C* **7**, 1046 (1974).
 - [3] R. Gupta, J. Delapp, G. G. Batrouni, G. C. Fox, C. F. Baillie, and J. Apostlakis, *Phys. Rev. Lett.* **61**, 1996 (1988).
 - [4] U. Wolff, *Nucl. Phys. B* **322**, 759 (1989).
 - [5] R. Gupta and C. F. Baillie, *Phys. Rev. B* **45**, 2883 (1992).
 - [6] Enzo Granato and M. P. Nightingale, *Phys. Rev. B* **48**, 7438 (1993).
 - [7] S. Lee and K. Lee, *Phys. Rev. B* **49**, 15 184 (1994).
 - [8] P. Olsson, *Phys. Rev. Lett.* **75**, 2758 (1995).
 - [9] Jorge V. José and G. Ramirez-Santiago, *Phys. Rev. Lett.* **77**, 4849 (1996).
 - [10] P. Olsson, *Phys. Rev. Lett.* **77**, 4850 (1996).
 - [11] H. K. Janssen, B. Schaub, and B. Schmittmann, *Z. Phys. B* **73**, 539 (1989).
 - [12] D. A. Huse, *Phys. Rev. B* **40**, 304 (1989).
 - [13] D. Stauffer, *Physica A* **186**, 197 (1992).
 - [14] Z. B. Li, U. Ritschel, and B. Zheng, *J. Phys. A* **27**, L837 (1994).
 - [15] P. Grassberger, *Physica A* **214**, 547 (1995).
 - [16] L. Schülke and B. Zheng, *Phys. Lett. A* **204**, 295 (1995).
 - [17] S. N. Majumdar, A. J. Bray, S. Cornell, and C. Sire, *Phys. Rev. Lett.* **77**, 3704 (1996).
 - [18] M. Krech, *Phys. Rev. E* **55**, 668 (1997).
 - [19] B. Zheng, *Int. J. Mod. Phys. B* **12**, 1419 (1998), review article.
 - [20] Z. B. Li, L. Schülke, and B. Zheng, *Phys. Rev. E* **53**, 2940 (1996).
 - [21] L. Schülke and B. Zheng, *Phys. Lett. A* **215**, 81 (1996).
 - [22] J. F. F. Mendes and M. A. Santos, *Phys. Rev. E* **57**, 108 (1998).
 - [23] P. Marcq and H. Chaté, *Phys. Rev. E* **57**, 1591 (1998).
 - [24] H. J. Luo, L. Schülke, and B. Zheng, *Phys. Rev. Lett.* **81**, 180 (1998).
 - [25] K. Okano, L. Schülke, and B. Zheng, *Phys. Rev. D* **57**, 1411 (1998).
 - [26] H. J. Luo and B. Zheng, *Mod. Phys. Lett. B* **11**, 615 (1997).
 - [27] L. W. Bernardi, S. Prakash, and I. A. Campbell, *Phys. Rev. Lett.* **77**, 2798 (1996).
 - [28] L. W. Bernardi and I. A. Campbell, *Phys. Rev. B* **56**, 5271 (1997).
 - [29] R. E. Blundell, K. Humayun, and A. J. Bray, *J. Phys. A* **25**, L733 (1992).